ACS APPLIED MATERIALS & INTERFACES

Research Article

www.acsami.org

Highly Efficient Monolithic Dye-Sensitized Solar Cells

Jeong Kwon,[†] Nam-Gyu Park,[†] Jun Young Lee,[†] Min Jae Ko,[*,§,⊥] and Jong Hyeok Park[*,†,‡]

[†]School of Chemical Engineering and [‡]SKKU Advanced Institute of Nanotechnology (SAINT), Sungkyunkwan University, Suwon 440-746, Republic of Korea

[§]Photo-Electronic Hybrids Research Center, Korea Institute of Science and Technology (KIST), Seoul 136-791, Korea

[⊥]Green School, Korea University, 145 Anam-ro, Seongbuk-gu, Seoul 136-701, Korea

Supporting Information

ABSTRACT: Monolithic dye-sensitized solar cells (M-DSSCs) provide an effective way to reduce the fabrication cost of general DSSCs since they do not require transparent conducting oxide substrates for the counter electrode. However, conventional monolithic devices have low efficiency because of the impediments resulting from counter electrode materials and spacer layers. Here, we demonstrate highly efficient M-DSSCs featuring a highly conductive polymer combined with macroporous polymer spacer layers. With M-DSSCs based on a PEDOT/polymer spacer layer, a power conversion efficiency of 7.73% was achieved, which is, to the best of our knowledge, the highest efficiency for M-DSSCs to date. Further, PEDOT/polymer spacer layers were applied to flexible DSSCs and their cell performance was investigated.

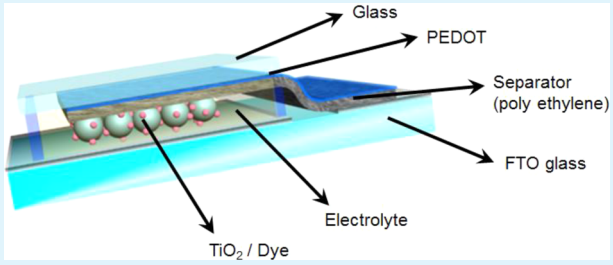

KEYWORDS: *dye-sensitized solar cells, monolithic, TCO less counter electrode, Pt free, flexible*

INTRODUCTION

Dye-sensitized solar cells (DSSCs) with a network of interconnected TiO_2 nanoparticles with dye molecules are currently attracting widespread scientific and commercial interest since these cells present a cheap and highly efficient alternative to conventional inorganic-based solar cells.[1] Since the study by Gräztel and O'Regan, DSSCs have been researched over the last 20 years.[2] In recent years, rapid development of DSSCs has been observed and an overall efficiency of ~12% has been reported.[3] Moreover, DSSCs are more environment friendly than other photovoltaic devices from the viewpoints of materials and processing conditions. These advantages make DSSCs an attractive renewable power source in the near future.

Typically, DSSCs are fabricated with two different electrodes, with a layer of transparent conducting oxide (TCO)-coated glass as the base; this type of structure is the so-called sandwich construction, i.e. the TiO_2 working electrode is applied on one of the substrates whereas the Pt counter electrode is on the other substrate.[4] The TCO glass is one of the most expensive components in DSSCs. Thus, the use of TCO glass makes the commercial production of DSSCs especially difficult. As an alternative structure, so-called monolithic designs have been proposed to solve the aforementioned obstacle. The monolithic DSSCs (M-DSSCs) differ from general DSSCs in that they are fabricated on a single TCO substrate, thus requiring only half the amount of TCO in theory. Typical M-DSSCs are composed of a mesoporous TiO_2 nanocrystal electrode on a transparent fluorine-doped tin oxide (FTO) substrate, an inorganic spacer layer, and a carbon-based counter electrode. The operating mechanism is exactly same as that of general DSSCs. However, M-DSSCs differ from the general DSSCs in that instead of a TCO substrate coated with Pt as the counter electrode used to reduce the tri-iodides, the carbon based materials act as both the charge conductor and the catalyst for reducing the electrolyte.[5]

M-DSSCs have the advantages of being cost-effective and have a simpler manufacturing process. However, their design and materials have not been extensively investigated for their commercialization potential. Because the general DSSCs and M-DSSCs have the exact similar photoanodes, they have to show comparable cell efficiency. However, most M-DSSCs cannot achieve more than 7.6% efficiency even after using platinized carbon counter material.[5] Given that carbon-based materials do not have conductivity and catalytic ability comparable to those of commercialized TCO/Pt, there is still room for improvement in cell efficiency by adapting new materials and device structures. First, we analyzed the disadvantages of M-DSSCs: (1) The carbon-based counter electrode is too thick to attain adequate conversion efficiency and it is also not suitable for flexible type DSSCs. (2) Carbon-based counter electrodes have not been shown to have cell performance comparable with that of conventional DSSCs. (3) The spacer layers for M-DSSCs have not been optimized. Generally, inorganic insulators composed of inorganic sub-micrometer sized particulate films have been used.[6−9]

Received: December 5, 2012
Accepted: February 22, 2013
Published: February 22, 2013

In the present work, a macroporous polymer membrane coated with a highly conductive polymer is employed not only as the spacer layer but also as the conductive/catalytic layer for the M-DSSC. The flexible characteristics of this unique material are appealing for the commercialization of M-DSSCs because lightweight, thin, and low-cost DSSCs can be fabricated by roll-to-roll mass production techniques. Moreover, a power conversion efficiency of 7.73% was achieved using the counter electrode, which is, to the best of our knowledge, the highest efficiency for M-DSSCs to date.

EXPERIMENTAL SECTION

Synthesis of PEDOT. The monomer solution was prepared by dissolving 0.2 g of 3,4-ethylenedioxythiophene (EDOT), 0.02 g of poly(vinyl pyrrolidone) as a matrix polymer, and 0.1 g of pyridine as a retardant in 2 mL of butanol. An oxidant solution was separately prepared by dissolving 2.38 g of ferric *p*-toluene sulfonate (FTS) in ethanol (45 vol %). The monomer and oxidant solutions were then mixed together, followed by solution polymerization at 70 °C for 20 min.[11,12] The prepolymerized PEDOT solution was then spin-coated onto the m-PE to form a prepolymerized PEDOT film, as can be seen in Figure 1b. The m-PE/PEDOT film was obtained by postpolymerization at 70 °C for 20 min, followed by washing with methanol and drying, resulting in a film. To control the thickness of the PEDOT on the m-PE spacer, we repeated the above procedure one to five times.

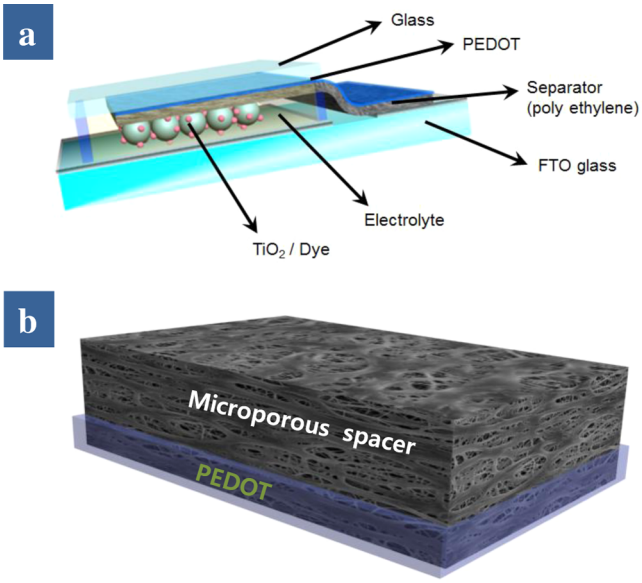

Figure 1. (a) Device configuration of monolithic DSSCs using (b) PEDOT-coated m-PE films.

Solar Cell Fabrication and Characterization. M-DSSCs were created using the screen-printing technique on pre-etched FTO master plates. The glass was cleaned by sonicating in dilute cuvette cleaning solution, distilled water, and then ethanol. Nanocrystalline TiO_2 particles were synthesized via a sol–gel hydrolysis process and autoclaving of titanium isopropoxide at 230 °C for 12 h in aqueous acetic acid solution, as described elsewhere.[10] The *n*-TiO_2 particles were dispersed in α-terpinol with ethyl cellulose as a binder. A spin-coating method using 100 mM Ti-isoproxide (Aldrich) was applied to form a thin TiO_x underlayer on fluorine-doped SnO_2 (FTO, TEC-15, Pilkington) glass. Thereafter, the *n*-TiO_2 electrodes were prepared by printing on the FTO substrate. After heat treatment at 550 °C for 30 min, the *n*-TiO_2 electrodes were immersed in 50 mM N719 solution. Counter electrodes were prepared by coating a PEDOT layer on the PE spacer film as described in the Results section. For preparation of the conventional DSSC, other counter electrodes were prepared by applying a drop of H_2PtCl_6 on the FTO glass followed by heating at 400 °C for 15 min. The samples were washed with ethanol and water sequentially and were dried for 2 h at 130 °C.

The dye-absorbed *n*-TiO_2 electrodes with the porous PE spacer with the PEDOT counter electrodes were assembled into sealed sandwich-type cells by heating with a hot melt of a polymer film (Surlyn, Dupont 1702). The electrolyte was composed of 0.6 M butylmethylimidazolium iodide, 0.03 M I_2, 0.1 M guanidinium thiocyanate, and 0.5 M 4-*tert*-butylpyridine in a mixture of acetonitrile and valeronitrile (v/v, 85:15).

Measurement. The *J*–*V* curves were measured at AM 1.5 illumination using a Keithley 2400 source measurement unit. A 1000 W xenon lamp (Oriel, Sol 3A) served as the light source and its intensity was calibrated using a Si reference cell (NREL-calibrated Si solar cell equipped with a KG-2 filter). IPCE was measured at a low chopping speed of 5 Hz using a system from PV Measurement, Inc., equipped with a halogen source and a broad band bias light for approximating one sun intensity. The IPCE system was calibrated using a silicon reference photodiode (G587, PV Measurement, Inc.).

RESULTS AND DISCUSSION

The M-DSSC shown in Figure 1 has a photoanode composed of FTO/glass substrate or In-doped tin oxide (ITO)/polyethylene naphthalate (PEN) coated with mesoporous TiO_2. The mesoporous TiO_2 layer is sensitized with ruthenium dye (N719) and functions as a photon-absorbing layer, and a macroporous polyethylene (m-PE) membrane acts as a spacer between the photoanode and the counter electrode. Conventional graphite/carbon black materials-based M-DSSCs have poor performance because of the low conductivity, high resistance, and poor catalytic activity of such materials. To overcome these limitations, highly conductive poly(3,4-ethylenedioxythiophene) (PEDOT) as the counter electrode was fabricated on the m-PE spacer layer by a modified simple presolution/in situ polymerization method, as reported elsewhere.[11]

Commercialized m-PE separators have appropriate pore size (~100 nm) and pore distribution that enables them to play a role in ion conduction in lithium ion rechargeable batteries.[13] Figure 2 shows scanning electron microscopic (SEM) images of the PEDOT-coated PE membrane spacer whose morphology is influenced by the thickness of the PEDOT thin film, which is in turn controlled by varying the number of spin-coating cycles. The SEM images show the changes in the pore structure of the PE spacer as a function of the number of spin-coating cycles. As the number of cycles is increased, the pores of the PE spacer are gradually filled. From the SEM images, it can be confirmed that the PEDOT layer generated by the polymerization method is stacked well on the surface of the PE spacer. Moreover, a uniform porous structure on the opposite side of the PE spacer was still observed even after 5 spin-coating repetitions (Supporting Information Figure S1).

Supporting Information Figure S2 shows the wetting behavior after several drops of the electrolyte were placed on the PE spacer surface. Generally, a polyolefin spacer intrinsically has strong hydrophobic characteristics and low ability to hold organic solvent, since it is poorly compatible with liquid electrolytes. Figure S2 confirms that the PE spacer is highly effective in absorbing the iodine/iodide liquid electrolyte, which facilitates the effective movement of ions in the electrolyte between the photoanode and the PEDOT counter electrode. This superior wetting behavior may induce the liquid electrolyte to infiltrate preferentially through the well-connected interstitial fiber voids and make contact with the PEDOT layer.

The photovoltaic characteristics for M-DSSCs are shown in Figure 3. These results show that the characteristics of the *J*–*V*

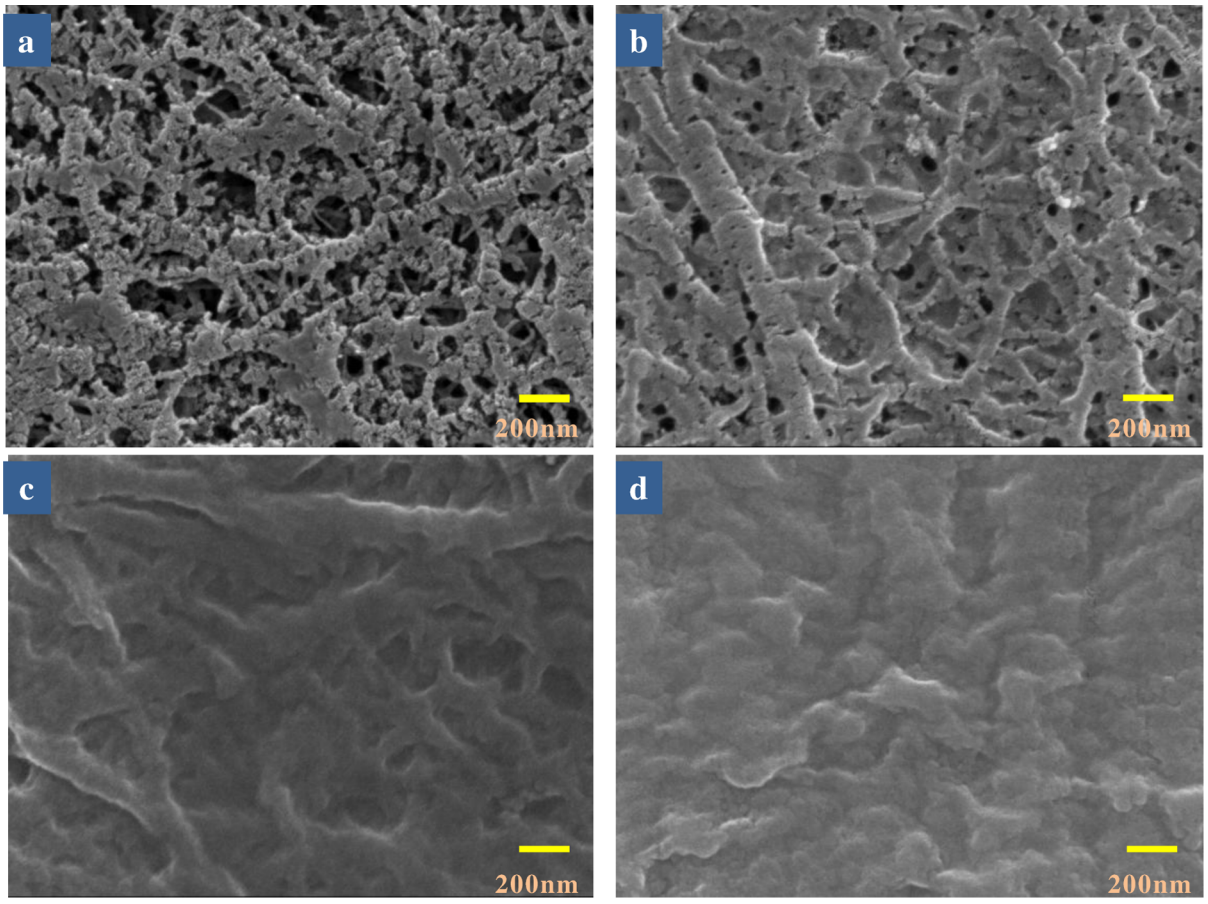

Figure 2. SEM images of the m-PE spacer layer coated with PEDOT: (a) bare m-PE film and the m-PE film coated with PEDOT (b) once, (c) twice, and (d) three times.

curves of M-DSSCs improve and approach those of conventional DSSCs as the thickness of the PEDOT layer on the m-PE spacer increases (Table 1). Because the PEDOT layer should act not only as the catalyst to reduce the tri-iodide, but also as the charge collector, we first investigated the catalytic functions of the PEDOT layer as a function of its thickness using conventional devices. To diminish one of the functions of the PEDOT (charge conductor), the counter electrode was prepared with a PEDOT coated FTO substrate. As seen in Supporting Information Figure S3, no serious deviations were observed in the $J-V$ characteristics with the thickness of the PEDOT layer. Thus, the thickness dependency on the cell performance in M-DSSCs can be attributed to the decreased resistance as the thickness of the PEDOT layer is increased on the m-PE spacer. However, the cell performance of the M-DSSC was not further improved beyond 4 cycles of deposition. When the 3-layered PEDOT was coated onto a glass substrate, the resulting surface conductivity was around 900 S/cm.

In M-DSSCs, the spacer layer, which lies between the TiO_2 photoanode and the PEDOT counter electrode, can act as the supporting substrate for the thin PEDOT layer. At the same time, the liquid electrolyte has to pass through freely to obtain sufficient ion mobility. This means the thickness of the insulating spacer layer is critical for device performance. The $J-V$ characteristics for two sets of devices were studied to compare the effects of the thickness of the m-PE spacer layer (Figure 3c and Table 2). When the 9-μm-thick PE spacer was coupled with three layers of PEDOT (~120 nm thickness) as a counter electrode, the cell efficiency was much higher than that

Table 1. Short-Circuit Current (J_{sc}), Open Circuit Voltage (V_{oc}), Fill Factor (FF), and Power Conversion Efficiency for M-DSSCs of Different PEDOT Coating Numbers

sample	J_{sc} (m A/cm^2)	V_{oc} (V)	FF (%)	eff (%)
PEDOT 1 layer	10.97	0.73	53.02	4.24
PEDOT 2 layers	12.74	0.74	51.44	4.86
PEDOT 3 layers	13.14	0.73	60.13	5.79
PEDOT 4 layers	12.68	0.72	59.95	5.50

Table 2. Short-Circuit Current (J_{sc}), Open Circuit Voltage (V_{oc}), Fill Factor (FF), and Power Conversion Efficiency for M-DSSCs with Different Spacer Layers

sample	J_{sc} (m A/cm^2)	V_{oc} (V)	FF (%)	eff (%)
15 μm spacer layer	13.14	0.73	60.13	5.79
9 μm spacer layer	15.19	0.77	66.22	7.73

of the M-DSSC with the 15-μm-thick PE spacer. Figure 3d shows the enhancement of J_{sc} in the presence of a thinner spacer film. The maximum value of IPCE for DSSCs occurs at around 540 nm, which corresponds to the absorption peak for N719. This indicates that the 9-μm spacer layer has higher efficiency than the 15-μm spacer layer in M-DSSCs. To investigate the effect of the spacer film thickness on cell performance, the ionic resistance of the m-PE spacers was measured at room temperature. The ionic resistance of the 9-μm-thick m-PE with 0.8 × 0.8 cm area was 0.78 Ω, while that of the 15-μm-thick m-PE with the same area was 1.3 Ω. In general,

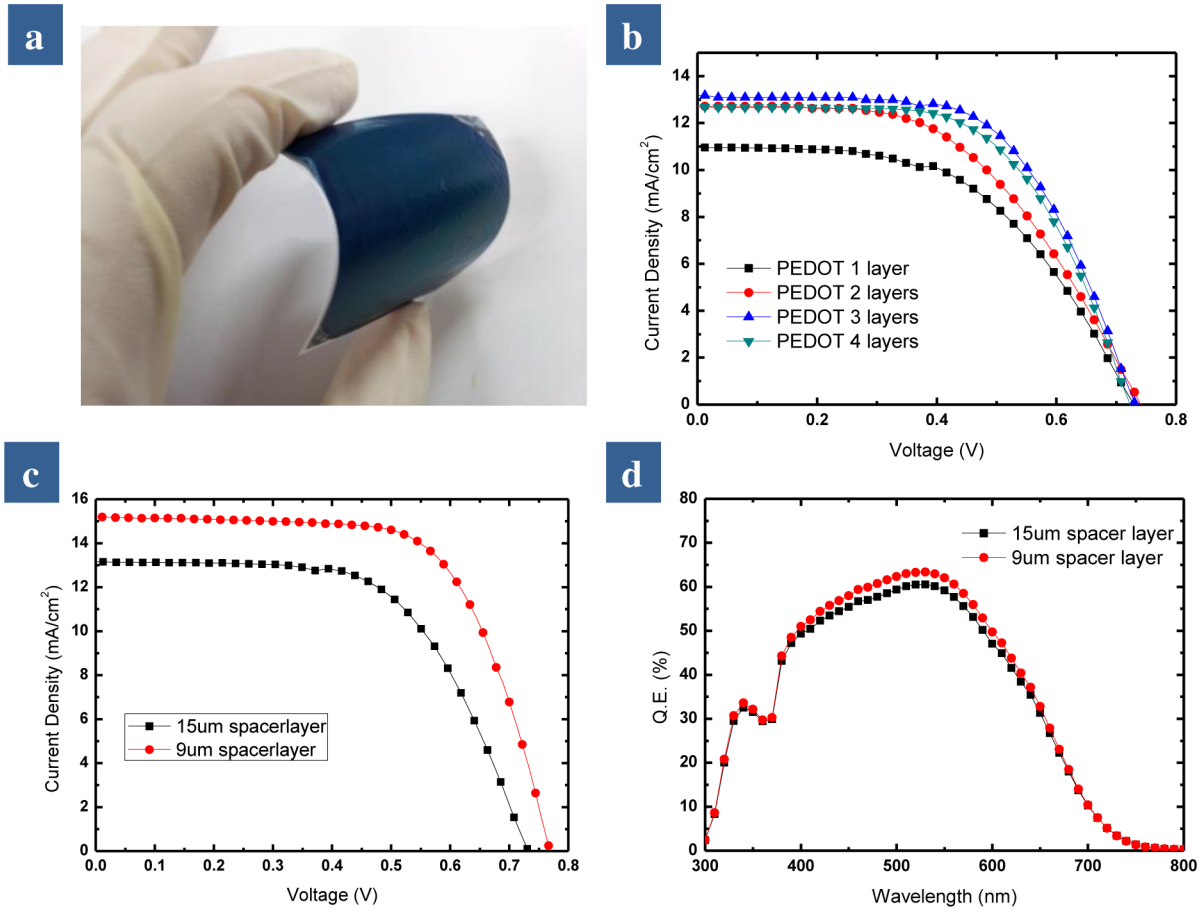

Figure 3. (a) Photograph of PEDOT/m-PE wetted with the electrolyte. (b) *J*–*V* curves of the monolithic DSSCs of different PEDOT coating numbers. (c) *J*–*V* curves and (d) IPCE of the monolithic DSSCs with different spacer layers.

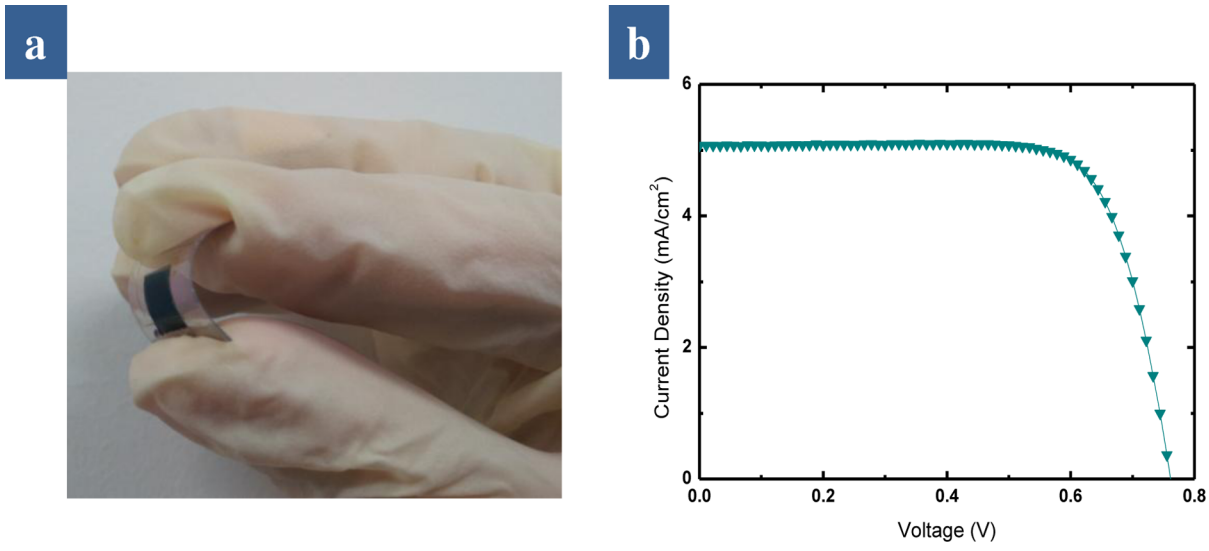

Figure 4. (a) Photograph of a flexible M-DSSC and (b) its *J*–*V* curve.

a Nyquist plot for a DSSC consists of two or three semicircles, with the first semicircle in the high frequency region attributed to an interfacial charge transfer process at the counter electrode, second semicircle in the mid frequiency region from TiO_2/dye/electrolyte charge transfer and third semicircle representing electrolyte diffusion. As can be seen in Supporting Information Figure S4, the total resistance of M-DSSC with the 9-μm-thick m-PE is much lower than that of M-DSSC with the 15-μm-thick m-PE.

Recently, flexible DSSCs have attracted great interest because they are lightweight, flexible, and cost efficient. Because of the highly flexible nature of the PEDOT coated m-PE film as shown in Figure 3a, we believe that the free-standing PEDOT film on the m-PE film is more suitable for flexible DSSCs owing

dx.doi.org/10.1021/am302974z | *ACS Appl. Mater. Interfaces* 2013, 5, 2070–2074

to the difficulty in preparing a flexible spacer layer using an inorganic particle film. Figure 4a shows a photograph of a flexible M-DSSC with the PEDOT coated m-PE film as the counter electrode. The $J-V$ characteristics of a flexible M-DSSC are also shown in Figure 4b. Under standard testing conditions, the flexible M-DSSC cell gave a photocurrent of 5.07 mA/cm^2, an open circuit voltage of 761.4 mV, and a fill factor of 0.7575, yielding a 3.0% conversion efficiency.

CONCLUSIONS

We fabricated highly efficient PEDOT-based monolithic DSSCs with polyethylene spacer layers. In comparison with carbon black/graphite-based devices, the cells with PEDOT showed a high efficiency of 7.73%, which is the best efficiency to date of monolithic DSSCs. This design for a PEDOT-based monolithic DSSC with a polyethylene spacer layer presents a promising substitute for conventional monolithic DSSCs and makes possible the low-cost commercial development of DSSCs.

ASSOCIATED CONTENT

Supporting Information

Additional SEM image, photograph, $J-V$ characteristics, and impedance data. This material is available free of charge via the Internet at http://pubs.acs.org.

AUTHOR INFORMATION

Corresponding Author

*E-mail address: lutts@skku.edu (J.H.P.), mjko@kist.re.kr (M.J.K.).

Notes

The authors declare no competing financial interest.

ACKNOWLEDGMENTS

This work was supported by NRF grants funded by the Korea Ministry of Education, Science and Technology (MEST) (2011-0030254, 2009-0092950, Pioneer Research Program (2012-0005955), Future-based Technology Development program (2010-0029321)). N.G.P. acknowledges the New and Renewable Energy Program through the KETEP funded by the Ministry of Knowledge Economy (MKE) (008NPV08J010000). M.J.K. acknowledges 2012 University-Institute Program funded by the National Research Foundation under the Ministry of Education, Science and Technology, Korea. J.H.P. acknowledges the support from the MKE (20123010010070).

REFERENCES

(1) Wang, P.; Zakeeruddin, S. M.; Comte, P.; Exnar, I.; Grätzel, M. *J. Am. Chem. Soc.* **2003**, *125*, 1166.
(2) O'Regan, B.; Grätzel, M. *Nature* **1991**, *353*, 737.
(3) Chen, C. Y.; Wang, M.; Li, J. Y.; Pootrakulchote, N.; Alibabaei, L.; Ngoc-le, C.; Decoppet, J. D.; Tsai, J. H.; Grätzel, C.; Wu, C. G.; Zakeeruddin, S. M.; Grätzel, M. *ACS Nano* **2009**, *3*, 3103.
(4) Lee, K. S.; Kwon, J.; Im, J. H.; Lee, C. R.; Park, N. G.; Park, J. H. *ACS App. Mater. Interfaces* **2012**, *4*, 4164.
(5) Liu, G.; Wang, H.; Li, X.; Rong, Y.; Ku, Z.; Xu, M.; Liu, L.; Hu, M.; Yang, Y.; Xiang, P.; Shu, T.; Han, H. *Electrochim. Acta* **2012**, *69*, 334.
(6) Hinsch, A.; Behrens, S.; Berginc, M.; Bönnemann, H.; Brandt, H.; Drewitz, A.; Einsele, F.; Faßler, D.; Gerhard, D.; Gores, H.; Haag, R.; Herzig, T.; Himmler, S.; Khelashvili, G.; Koch, D.; Nazmutdinova, G.; Opara-Krasovec, U.; Putyra, P.; Rau, U.; Sastrawan, R.; Schauer, T.; Schreiner, C.; Sensfuss, S.; Siegers, C.; Skupien, K.; Wachter, P.; Walter, J.; Wasserscheid, P.; Würfel, U.; Zistler, M. *Prog. Photovolt: Res. Appl.* **2008**, *16*, 489.
(7) Ito, S.; Takahashi, K. *Nature Photon.* **2008**, *2*, 693.
(8) Kay, A.; Grätzel, M. *Solar Energy Mater. Solar Cells* **1996**, *44*, 99.
(9) Murakami, T. N.; Ito, S.; Wang, Q.; Nazeeruddin, M. K.; Bessho, T.; Cesar, I.; Liska, P.; Humphrybaker, R.; Comte, P.; Péchy, P.; Grätzel, M. *J. Electrochem. Soc.* **2006**, *153*, A2255.
(10) Wang, P.; Zakeeruddin, S. M.; Comte, P.; Charvet, R.; Humphry-Baker, R.; Grätzel, M. *J. Phys. Chem. B* **2003**, *107*, 14336.
(11) Lee, K. S.; Lee, H. K.; Wang, D. H.; Park, N. G.; Lee, J. Y.; Park, O. O.; Park, J. H. *Chem. Commun.* **2010**, *46*, 4505.
(12) Lee, K. S.; Lee, Y.; Lee, J. Y.; Ahn, J. H.; Park, J. H. *ChemSusChem* **2012**, *5*, 379.
(13) Zhang, S. S. *J. Power Sources* **2007**, *164*, 351.